Two Separate One-Electron Steps in the Reductive Activation of the A Cluster in Subunit β of the ACDS Complex in *Methanosarcina thermophila*[†]

Simonida Gencic and David A. Grahame*

Department of Biochemistry and Molecular Biology, Uniformed Services University of the Health Sciences, Bethesda, Maryland 20814-4799

Received December 7, 2007; Revised Manuscript Received March 10, 2008

ABSTRACT: Acetyl-CoA decarbonylase/synthase (ACDS) is a multienzyme complex found in methanogens and certain other Archaea that carries out the overall synthesis and cleavage of the acetyl C−C and C−S bonds of acetyl-CoA. The reaction is involved both in the autotrophic fixation of carbon and in the process of methanogenesis from acetate, and takes place at a unique active site metal center known as the A cluster, located on the beta subunit of the ACDS complex and composed of a binuclear Ni−Ni site bridged by a cysteine thiolate to an Fe_4S_4 center. In this work, a high rate of acetyl-CoA synthesis was achieved with the recombinant ACDS beta subunit by use of methylcobinamide as an appropriate mimic of the physiological base-off corrinoid substrate. The redox dependence of acetyl-CoA synthesis exhibited one-electron Nernst behavior, and the effects of pH on the observed midpoint potential indicated that reductive activation of the A cluster also involves protonation. Initial burst kinetic studies indicated the formation of stoichiometric amounts of an A cluster-acetyl adduct, further supported by direct chromatographic isolation of an active enzyme-acetyl species. Titration experiments indicated that two electrons are required for activation of the enzyme in the process of forming the enzyme-acetyl intermediate. The results also established that the A cluster-acetyl species undergoes reductive elimination of the acetyl group with the simultaneous release of two, low potential electron equivalents. Thus, the one-electron Nernst behavior can be interpreted as the sum of two separate, low potential, one-electron steps. The results tend to exclude reaction mechanisms involving either one- or three-electron reduced forms of the A cluster as immediate precursors to the acetyl species. A scheme involving a $[Fe_4S_4]^{1+}$-Ni^{1+} species is favored over a $[Fe_4S_4]^{2+}$-Ni^0 form. The role of proton uptake in the possible formation of a Ni^{2+}-hydride intermediate is also discussed. Trapping of electrons during the formation of the A cluster-acetyl species from substrates CO and methylcobinamide was found to be highly favorable, thus presenting a means for extensive activation of the enzyme under otherwise nonpermissive physiological redox potentials.

In methanogens and certain other species of Archaea the direct synthesis and cleavage of the acetyl C−C bond of acetyl-CoA is catalyzed by the acetyl-CoA decarbonylase/synthase (ACDS[1]) multienzyme complex. With a total molecular mass of ca. 2,000 kDa, the complex contains five subunits in a probable oligomeric structure of $(\alpha_2\varepsilon_2)_4\beta_8(\gamma\delta)_8$. The ACDS complex is indispensable for autotrophic growth of hydrogen-consuming methanogens and for methanogens growing on C-1 substrates, such as methylsulfides, methylamines and methanol, because it supplies the only source of 2-carbon units available for anabolic processes (*1, 2*). In *Archaeoglobus fulgidus*, ACDS is used in the complete oxidation of acetate to 2 CO_2, a process coupled to sulfate reduction and energy transduction (*3*). Moreover, ACDS occupies a central position in the major catabolic pathway of acetate degradation to methane and CO_2 carried out by species of Methanosaeta and Methanosarcina. The ACDS complex catalyzes the overall reaction given in eq 1

$$\text{acetyl-CoA} + H_4\text{SPt} + H_2O + 2Fd_{ox} \rightleftarrows \text{CoASH} + CH_3\text{-}H_4\text{SPt} + CO_2 + 2Fd_{red} + 2H^+ \quad (1)$$

in which H_4SPt stands for tetrahydrosarcinapterin (a tetrahydrofolate analogue that acts as acceptor of the methyl group derived from acetyl C−C cleavage), and Fd represents ferredoxin, the physiological acceptor of electrons produced by oxidation of the carbonyl group of acetyl-CoA to CO_2 (*4, 5*). Partial proteolytic dissociation of the complex led to the isolation of three separate metalloprotein subcomponents: a Ni- and Fe/S-containing CO dehydrogenase ($\alpha_2\varepsilon_2$), a corrinoid Fe/S component ($\gamma\delta$) with truncation of the δ N-terminus, and a modified form of the β subunit truncated at the C-terminus. Furthermore, the roles of these protein subcomponents have been identified in catalyzing different

[†] This work was supported by grants from the National Science Foundation (MCB-0215160) and by the U.S. Department of Energy (DE-FG02-00ER15108).

* To whom correspondence should be addressed. Department of Biochemistry and Molecular Biology, Uniformed Services University of the Health Sciences, 4301 Jones Bridge Rd., Bethesda, MD 20814-4799. Tel: 301-295-3555. Fax: 301-295-3512. E-mail: dgrahame@usuhs.mil.

[1] Abbreviations: ACDS, acetyl-CoA decarbonylase/synthase; CODH, carbon monoxide dehydrogenase; H_4SPt, tetrahydrosarcinapterin; CH_3-H_4SPt, N^5-methyltetrahydrosarcinapterin; HEPES, *N*-2-hydroxyethylpiperazine-*N*′-2-ethanesulfonic acid; IPTG, isopropyl β-D-thiogalactopyranoside; MOPS, 3-(*N*-morpholino)propanesulfonic acid; NTA, nitrilotriacetate, TCEP, *tris*(2-carboxyethyl)phosphine hydrochloride.

10.1021/bi7024035 CCC: $40.75
Published on Web 04/29/2008

Scheme 1: Structural Model of the A Cluster

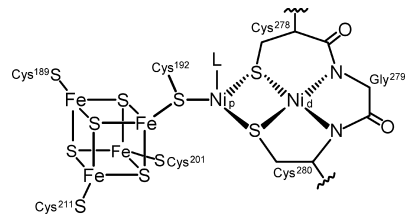

partial reactions in the overall synthesis and cleavage of acetyl-CoA (*6*).

Acetyl-CoA binding takes place on the ACDS β subunit, and, at low redox potentials the acetyl group is transferred to the protein, releasing CoA and forming an acetyl-enzyme species in which the thioester transfer potential from acetyl-CoA is preserved, activating the acetyl group for C−C bond scission in the acetyl-enzyme complex (*7*), as shown in eq 2, where E_β stands for the reduced β subunit.

$$E_\beta + \text{acetyl-CoA} \rightleftarrows E_\beta\text{-acetyl} + \text{CoA} \quad K'_{eq} \approx 0.2 \qquad (2)$$

Measurements of the redox potential dependence of acetyl transfer activity indicated an apparent one-electron process for reductive activation of the enzyme (*7*), in agreement with studies on the CoA exchange reaction catalyzed by bacterial CO dehydrogenase/acetyl-CoA synthase (CODH/ACS) (*8*), a bifunctional 310 kDa $\alpha_2\beta_2$ heterotetramer involved in acetate synthesis in the acetogen *Moorella thermoacetica*. Cleavage of the enzyme acetyl C−C bond generates CO and a methyl group that is then transferred to the corrinoid cofactor of the $\gamma\delta$ protein subcomponent. A second transfer of the methyl group from the corrinoid cofactor to the substrate H_4SPt follows, rapidly forming CH_3-H_4SPt according to eq 3.

$$E_{\gamma\delta}\text{-}CH_3\text{-Co(III) corrinoid} + H_4\text{SPt} \rightleftarrows E_{\gamma\delta}\text{-Co(I) corrinoid} + CH_3\text{-}H_4\text{SPt} + H^+ \qquad (3)$$

The final oxidation of the carbonyl group of acetyl-CoA is catalyzed by the $\alpha_2\varepsilon_2$ CO dehydrogenase component (eq 4).

$$CO + H_2O \rightleftarrows CO_2 + 2H^+ + 2e^- \qquad (4)$$

Studies on native and recombinant forms of the ACDS β subunit indicate that acetyl C−C and C−S bond activation occur at an active site metal center, the A cluster, composed of a binuclear Ni−Ni center bridged to an $[Fe_4S_4]$ cluster. The structure of the A cluster shown in Scheme 1 is based on results from X-ray crystallographic studies on the bacterial CODH/ACS enzyme (*9*−*11*) and is supported by site-directed mutagenesis, Ni reconstitution measurements, Ni and Fe XANES, Ni and Fe EXAFS, Ni L-edge, and XMCD spectroscopy of the recombinant ACDS β subunit (*12*−*14*). The Ni-reconstituted recombinant β subunit exhibits redox potential-dependent acetyl transferase activity at rates comparable to those of the native enzyme. In addition, net synthesis of acetyl-CoA from CoA, CO, and methylcobalamin was detected with the β subunit in the absence of all other ACDS protein subunits. However, the rate of this reaction was only approximately 1/3000th of the rate catalyzed by the intact ACDS complex using CoA, CO, and CH_3-H_4SPt as substrates. Other properties of the Ni reconstituted recombinant protein were essentially identical to those found with the native ACDS complex or the isolated β subunit, including the formation of the NiFeC species EPR signal upon reaction with CO, and a Fe:Ni composition ratio of 2:1 (*12*).

Mechanisms proposed for acetyl C−C bond formation and cleavage at the A cluster involve organometallic intermediates, i.e., acetyl-Ni, methyl-Ni, and Ni-CO species, formed by the reaction of substrates with Ni_p at a low-valence state (*12, 15*−*22*). A step in which CO and CH_3 ligands combine to form a Ni^{2+}-acetyl species is envisaged, which would involve methyl group migration or carbonylation (with the reverse C−C bond fragmentation reaction proceeding by decarbonylation or migration of the methyl group in the opposite direction). There is general agreement that in the unreduced cluster the predominant oxidation state is Ni^{2+} for both Ni_p and Ni_d and that as a square-planar d^8 ion, Ni_d remains in the 2+ state throughout the catalytic cycle. However, differences exist in the assignment of the Ni_p oxidation state in the active reduced form of the A cluster as either Ni^{1+} or Ni^0. There is also debate about the proposed order of the addition of substrates and as to whether or not the NiFeC species (formulated as Ni^{1+}-CO) is an inhibitor or actually part of the catalytic cycle (*12, 22, 23, 18*). Arguments have been made for a Ni^0-based mechanism on the basis of structure−reactivity correlations among various synthetic Ni-organometallic model complexes (*18*). Density functional theory computational studies have been applied, but results vary on whether reduction by two electrons would produce Ni^0 in proximity to $[Fe_4S_4]^{2+}$ (*19*) or result in a $[Fe_4S_4]^{1+}$-Ni_p^{1+} configuration (*24, 20*), which then could achieve the Ni_p^0 state by accepting a third electron to form $[Fe_4S_4]^{1+}$-Ni_p^0 (*20*). The one-electron Nernst behavior in the reductive activation of the ACDS β subunit has been interpreted as support for a mechanism involving Ni^{1+} (*12*), and as much as 30% of the Ni was assigned to Ni^{1+} in fitting the Ni L-edge spectrum of the enzyme reduced in the presence of Ti^{3+} citrate (*14*). A better knowledge of the number of electron equivalents required to activate the enzyme would yield insight into the redox state of Ni in the reduced A cluster and thereby advance the understanding of the reaction.

In this work, a high rate of acetyl-CoA synthesis on the same order of magnitude as that of the native enzyme complex is reported with the Ni reconstituted recombinant β subunit by use of a more reactive methyl group donor substrate methylcobinamide as a better mimic of the physiological corrinoid substrate. The redox dependence of overall acetyl-CoA synthesis activity is examined to assess whether it corresponds to the identical activation process as that previously observed in studies on acetyl transferase activity displaying one-electron Nernst behavior. The effect of pH on the observed midpoint potential for activation of acetyl-CoA synthesis is evaluated to explore the role of protonation in the reductive activation process. Conditions are developed to yield stoichiometric formation of an A-cluster acetyl species, and chromatographic isolation of the enzyme-acetyl form is employed to verify its stability. To establish the number of low potential electrons required for activation of the enzyme, quantification is made of the reducing equivalents taken up and released during formation and reductive elimination of the enzyme acetyl group. The one-electron Nernst behavior of reductive activation is concluded to result

from the sum of two separate low potential one-electron steps, one of which apparently is accompanied by the uptake of a proton. The results favor a mechanism involving a two-electron reduced form of the A cluster over either one- or three-electron reduced species in directly generating the A cluster-acetyl intermediate. The efficient trapping of two low potential equivalents observed during the formation of the enzyme-acetyl species under relatively mild potentials suggests a means for cluster activation under physiologically relevant reducing conditions.

MATERIALS AND METHODS

General Procedures and Reagents. Chemicals purchased from commercial sources were of the highest purity grade offered, and all aqueous solutions were prepared using deionized water (Milli-Q apparatus, Millipore Corp.). Coenzyme A, disodium salt (>96%, HPLC, Fluka BioChemika), and 1,1′-dibenzyl-4,4′-bipyridinium dichloride (benzyl viologen) were purchased from Sigma. Methyl viologen dichloride dihydrate, 98%, was from Aldrich, and *tris*(2-carboxyethyl)phosphine hydrochloride (TCEP) was from Calbiochem (EMD Biosciences). Anaerobic procedures were performed under an atmosphere of nitrogen containing 1−3% H_2 using a Coy-type anaerobic chamber, and O_2 levels were maintained in the range of 0.5−2 ppm, monitored by a Teledyne model 3190 trace oxygen analyzer. Titanium (III) nitrilotriacetate (Ti^{3+} NTA) stock solution, containing approximately 130 mM Ti^{3+}, was prepared fresh by adding 1 volume of 30% wt. titanium (III) chloride in 2 N HCl reagent (Acros) to 13.8 volumes of a solution containing 0.275 M nitrilotriacetate disodium salt, 0.5 M Tris-HCl at pH 8.0. Further dilutions with water provided working solutions in the range of 2−20 mM Ti^{3+} for direct additions to enzyme reaction mixtures. The exact concentration of Ti^{3+} was determined separately in spectrophotometric titrations with methyl viologen, using 13.1 mM^{-1} as the absorptivity coefficient at 600 nm of reduced methyl viologen (*25*). Titration of cob(II)alamin to cob(I)alamin with Ti^{3+} NTA at pH 7.2 indicated an apparent midpoint potential of the blue Ti^{3+} NTA complex around −610 mV, intermediate between the values of −480 mV and −750 mV for the purple Ti^{3+} EDTA and brown Ti^{3+} citrate forms, respectively (*7*).

Methylcobinamide. Methylcobinamide was prepared from methylcobalamin by the method developed in the laboratory of K.L. Brown (*26*), with all steps carried out in dim light or darkness. Methylcobalamin (Sigma), 0.10 g, dried over P_2O_5, was combined with 1.2 mL of trifluoromethanesulfonic acid, 99+%, (Aldrich), and magnetically stirred for 24 h in a sealed vial under dry nitrogen. The reaction mixture was then added to 200 mL 1 M Na_2HPO_4, allowed to stand overnight, and then desalted by pumping the solution onto a chain of five Sep-Pak C18 cartridges (Waters) connected in series, followed by water washing and elution with 50% methanol. Fractions were dried, redissolved in water, and portions were subjected to cation exchange chromatography on a 5-mL BioRad Econo-Pac High S Cartridge using isocratic elution with water followed by 20 mM sodium phosphate at pH 7.4. The pooled High S peak fractions were concentrated and desalted using Sep-Pak C18 cartridges. Seventy-seven percent of the material eluted from the cartridges was combined, dried, redissolved in anaerobic water, aliquoted and stored as a frozen stock solution of approximately 6.5 mM methylcobinamide. Gradient HPLC analysis of samples of the final preparation, carried out as described in ref *27*, indicated a purity of 97% based on absorbance monitored at 250 nm. Methylcobinamide concentration was calculated using a molar absorptivity coefficient of 10,700 $M^{-1}cm^{-1}$ at 462 nm (*28*).

Recombinant ACDS β Subunit. The expression vector pQE60-ΔHis encoding a C-terminally truncated form of the ACDS β subunit (CdhC*, mol mass 44,568) was used as described previously for heterologous expression in *E. coli* under strictly anaerobic conditions (*12*). Purification of the recombinant β subunit protein was carried out by anion exchange chromatography of *E. coli* extracts on Q Sepharose Fast Flow (GE Healthcare) as described previously (*12*), and followed by an additional step in which 2−3 mg samples (6.7 to 10 mg/mL) of the concentrated pool from Q Sepharose were applied to a Superose 12 HR 10/30 gel filtration column (GE Healthcare) and eluted with 10 mM HEPES and 190 mM KCl at pH 8.3. Ni reconstitution was performed by the addition of 0.15 mM $NiCl_2$ to a solution containing 50 mM KCl, 10 mM HEPES at pH 8.3, and ca. 2 mg/mL diafiltered protein from Superose 12 pools, followed by overnight incubation at room temperature, similar to the methods previously described (*12*). Protein determinations and ICP metal analyses were carried out as given in ref *12*, and the protein used here, as in previous studies, contained approximately 3 g-atom iron per mol CdhC*.

Chromatographic Isolation of the β Subunit-Acetyl Species. A reaction mixture (400 μL) containing 100 μM methylcobinamide, Ni reconstituted CdhC*, 33 μM, and 50 μM Ti^{3+} NTA in 50 mM HEPES buffer at pH 8.3 was incubated anaerobically at room temperature under a 100% CO atmosphere for 5 min and thereafter applied to a Superose 12 HR 10/30 gel filtration column. Elution was carried out at 0.5 mL/min with 10 mM HEPES and 190 mM KCl at pH 8.3, and UV−visible spectra were recorded on the effluent every 15 s using an HP 8452A spectrophotometer equipped with an 80 μL quartz cuvette flow cell set up inside the anaerobic chamber. Fractions were collected at 0.5 min intervals beginning 20 min after the reaction mixture was loaded. Immediately after each fraction was collected, 100 μM coenzyme A was added from a 5 mM stock solution. A sample, 200 μL, was then removed, mixed with 50 μL of stop solution (0.5 M sodium citrate at pH 4.0, containing 2 mM $TiCl_3$), and frozen in liquid nitrogen for subsequent quantification of acetyl-CoA and methylcobinamide in each fraction by HPLC analysis according to the method described previously (*7*).

Acetyl-CoA Synthesis Reactions. Acetyl-CoA synthesis from CoA, methylcobinamide, and CO was measured by following the conversion of methylcobinamide to cob(I)inamide spectrophotometrically and by direct quantification of acetyl-CoA production and CoA consumption by HPLC analysis of samples taken as a function of time. The reactions were set up inside the anaerobic chamber in either serum-stoppered glass vials or semimicro quartz cuvettes, in both cases fitted with inlet and outlet ports for exchanging the headspace with CO/N_2 gas mixtures. The 600 μL standard reaction was carried out at room temperature and contained 50 mM HEPES buffer at pH 7.2, 0.05 mM methylcobina-

mide, 25 μM Ti^{3+} NTA, Ni-reconstituted β subunit protein, 150 μL of CO saturated water, and 120 μM CoA. All components except CoA were mixed, and the headspace was replaced by purging with 25% CO and 75% N_2. The mixture was then preincubated for 5 min before starting the reaction by the addition of CoA. Aliquots removed by syringe at timed intervals were mixed with an equal volume of stop solution (0.5 M sodium citrate at pH 4.0, containing 2 mM $TiCl_3$), immediately frozen, and subsequently analyzed by HPLC (*7*). In reactions in which the order of addition of substrates was changed, a nitrogen atmosphere was present during preincubation, CO saturated water was added to initiate the reaction, and the headspace was flushed with the CO/N_2 gas mixture immediately thereafter.

Redox Buffer System. In calibration tests using potentiometric measurements with a gold electrode and a Ag/AgCl reference, a range of stable redox potentials could be obtained by adding varying amounts of Ti^{3+} NTA to bring about partial reduction of mixtures containing either 0.1 mM methyl viologen or 0.1 mM benzyl viologen. The observed potential values were well predicted from fits to the Nernst equation, eq 5,

$$E = E_0 + 2.303(RT/nF)\log(\mathrm{Viol_{ox}}/\mathrm{Viol_{red}}) \qquad (5)$$

in which $Viol_{red}$ (the concentration of reduced viologen) was determined as being equal to the concentration of Ti^{3+} NTA added, and $Viol_{ox}$ (the concentration of oxidized viologen) was obtained as total viologen minus $Viol_{red}$. For each of the two viologens, the E_0 and n parameters obtained from the fits agreed with published values (see Supporting Information, Figure S1). Reactions to determine the redox dependence of acetyl-CoA synthesis were set up according to the same procedure as for the standard reaction except that either 0.1 mM methyl viologen or 0.1 mM benzyl viologen was included along with varying amounts of Ti^{3+} NTA added prior to the 5 min preincubation period. The aliquot volumes of the Ti^{3+} NTA stock solution added were predetermined from the calibration trials to give the potentials indicated.

RESULTS

Rapid Synthesis of Acetyl-CoA Catalyzed by the ACDS β Subunit Using Methylcobinamide as a Base-Off Corrinoid Methyl Donor Substrate. In order to examine the effects of different corrinoid methyl donor substrates on the rate of acetyl-CoA synthesis, methylcobinamide, a corrinoid in which the lower axial ligand to Co is removed, i.e., base-off, was prepared and used in reactions containing the Ni reconstituted recombinant ACDS β subunit in the absence of all other ACDS protein components. Previous studies established that the β subunit protein by itself does form acetyl-CoA from CoA and CO in the presence of methylcobalamin (a base-on corrinoid); however, the reaction rates were very low (*12*). Reaction mixtures were set up containing the Ni reconstituted β subunit, CO and methylcobinamide, and were initiated by addition of CoA. As shown in Figure 1, spectrophotometric measurements indicated rapid consumption of CH_3-cob(III)inamide, quantitatively converting it to cob(I)inamide. HPLC analyses of aliquots removed from reaction mixtures verified the concomitant stoichiometric production of acetyl-CoA. Under conditions of low methylcobinamide concentration (Figure 1), acetyl-CoA synthesis exhibited an approximate first-order dependence on methylcobinamide concentration. Nearly equivalent rates were observed in reactions initiated with either 120 or 240 μM CoA, and no difference was found when the concentration of CO was varied by pre-equilibrating the reaction mixtures under either 25 or 50% CO in N_2. Changing the order of addition of substrates had only a minor effect on the reaction, such that when CO was added to start the reaction the rate was about 80% of that found when CoA was used. The reaction rate was not increased by increasing the concentration of reducing agent Ti^{3+} NTA or Ti^{3+} citrate in the range of 0.025 to 1 mM. (However, at 0.05 mM Ti^{3+} and higher, increasing amounts of an additional early peak were noted that coeluted with adenosine 3′,5′-diphosphate in HPLC profiles.) In the absence of Ti^{3+}, reactions initiated with CoA exhibited a short lag phase (less than 1 min) but otherwise had maximal rates that were essentially unchanged. An extensive lag was found under conditions in which the enzyme was preincubated with CoA in the absence of Ti^{3+}. The reaction did not start until Ti^{3+} was subsequently added, but thereafter immediately proceeded at a high rate. The lag was abolished by including 30 μM TCEP in the incubation mixture added together with 120 μM CoA. Likewise, the short lag in reactions initiated with CoA in the absence of Ti^{3+} was also eliminated when TCEP was similarly added to the CoA stock solution used to start the reaction. The effects of TCEP were consistent with the suppression of a slight oxidizing effect of the CoA preparation, perhaps due to the content of a small amount of CoA disulfide.

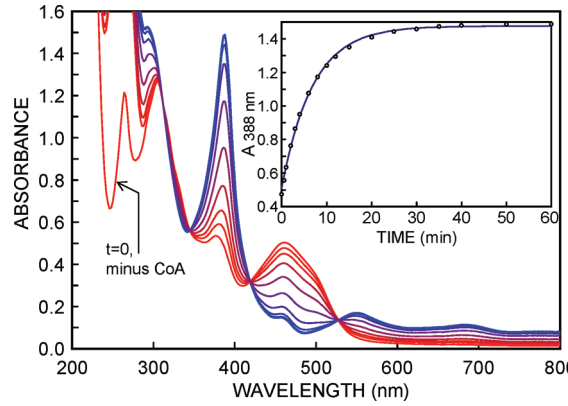

FIGURE 1: Rapid synthesis of acetyl-CoA catalyzed by the ACDS β subunit from carbon monoxide, CoA, and methylcobinamide. The reaction was set up as described under Materials and Methods for the standard reaction and contained 1.25 μM β subunit protein, 50 μM methylcobinamide, 240 μM CO, and 120 μM CoA at pH 7.2 and 25 °C. The reaction was initiated by the addition of CoA and the conversion of methylcobinamide to cob(I)inamide was followed spectrophotometrically. Spectra shown were recorded prior to CoA addition (t = 0, minus CoA) and thereafter at 0.5, 1, 2, 4, 8, 15, 25, 40, and 60 min. The inset shows a plot of the absorbance at 388 nm due to cob(I)inamide production fit to a simple first order rate equation.

The initial rate of acetyl-CoA synthesis was measured in reactions containing increasing amounts of methylcobinamide in the range of 0.05 to 0.8 mM. As shown in Figure 2, the reaction exhibited saturation behavior and was fit to the Michaelis−Menten equation yielding an apparent K_m of 0.533 +/− 0.056 mM and a V_{max} of 43.7 +/− 2.4 min^{-1} (turnover number). The value of V_{max} was approximately 30% of the turnover rate of the native *M. thermophila* ACDS

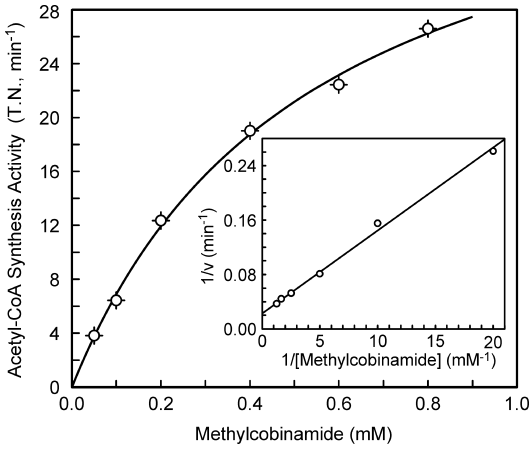

FIGURE 2: Effect of methylcobinamide concentration on the rate of acetyl-CoA synthesis by the ACDS β subunit. The standard reaction conditions were employed except that the total reaction volume was reduced to 100 μL and acetyl-CoA formation was measured by HPLC analysis of 10 μL aliquots removed over time. The data were fit directly to the Michaelis−Menten equation, and the inset shows the data plotted in double reciprocal format.

complex measured under the same conditions of pH, temperature, CO, and CoA concentration using the physiological methyl donor substrate CH_3-H_4SPt. By comparison, the ACDS complex exhibited only about one-half of the activity of the recombinant β subunit protein with 0.05 mM methylcobinamide used in the reaction.

Redox Dependence of Acetyl-CoA Synthesis. To assess the effect of redox potential on acetyl-CoA synthesis catalyzed by the ACDS β subunit, acetyl-CoA synthesis reactions were carried out at different redox potentials, established by including 0.1 mM methyl viologen or 0.1 mM benzyl viologen reduced to different levels, as described under Materials and Methods. HPLC analysis was used to measure the progress of the reactions rather than the spectrophotometric method because of the spectral interference from reduced viologen. The initial rate of acetyl-CoA synthesis in the redox buffered reactions was expressed as a percent of the total activity measured in the assay containing Ti^{3+} NTA in the absence of viologen[2], and is plotted versus potential, as shown in Figure 3A. The data from experiments at three different pH conditions were each fit to the Nernst equation, and the results showed that the midpoint potential for the activation of the enzyme became increasingly more negative as the pH was increased. At pH 6.58, 7.21, and 8.18, the best fit values of apparent E_0 were −463, −490, and −547 mV, with n = 1.07, 0.93, and 0.90 electron equivalents, respectively. The plot of the apparent E_0 versus pH (Figure 3B) had a slope of −53 mV/pH, indicating that the reductive activation of the enzyme involves the uptake of approximately one proton.

Initial Burst Formation of Acetyl-CoA and Stoichiometric Formation of an A Cluster Acetyl Intermediate. In the determination of the initial rates of acetyl-CoA formation at different redox potentials, a small but significant nonzero

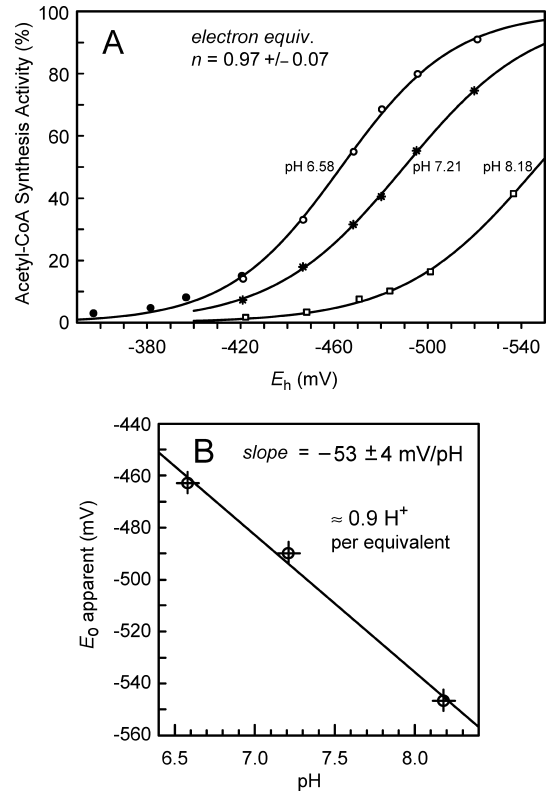

FIGURE 3: Reductive activation of acetyl-CoA synthesis at different pH and redox potentials. (A) Reactions were performed as described for the standard reaction except that 0.1 mM methyl viologen or 0.1 mM benzyl viologen (at potentials around −420 mV or higher, indicated by solid circles) was included and the amount of Ti^{3+} NTA was varied to obtain the indicated potentials (see Redox Buffer System under Materials and Methods). Activity of 100% corresponds to turnover rates of 1.90, 4.97, and 4.61 min^{-1}, at pH 6.58, 7.21, and 8.18, respectively. (B) The apparent midpoint potential for the activation of acetyl-CoA synthesis as a function of pH.

intercept was noted in the primary plots of acetyl-CoA HPLC peak area versus reaction time (see Supporting Information, Figure S2), which suggested that a small amount of acetyl-CoA may have been produced in the reactions immediately upon addition of CoA. The concentration of acetyl-CoA found was approximately equivalent to the concentration of β subunit protein used in the reactions. Therefore, to determine whether the initial amount of acetyl-CoA could be correlated with the amount of enzyme present, reaction mixtures were set up containing substantially larger quantities of the β subunit protein and carried out under pH and redox conditions designed to give relatively low turnover rates such that accurate values for the zero-time intercept could still be obtained. As shown in Figure 4A, increasing the concentration of the enzyme indeed resulted in an increase in the initial concentration of acetyl-CoA. A replot of the intercept versus enzyme concentration, fit by ordinary least-squares regression analysis, Figure 4B, yielded a value of the slope almost exactly equal to 1.0 mol acetyl-CoA formed per mol β subunit. Since no CoA or acetyl-CoA was detected by HPLC analysis of the enzyme preparation itself, i.e., in control reactions to which no CoA had been added, the results indicated that stoichiometric formation of an A cluster-acetyl species had taken place during the preincubation with CO and methylcobinamide, which upon addition of CoA was rapidly converted to acetyl-CoA.

[2] For the reactions at pH 8.18, the total activity was taken to be 1.32 times greater than the actual value of 3.50 min^{-1} measured in the absence of viologen. This improved the fit, which is reasonable because, in contrast to what was observed at pH 7.2, increasing concentrations of Ti^{3+} at the higher pH did give noticeably higher rates of acetyl-CoA synthesis.

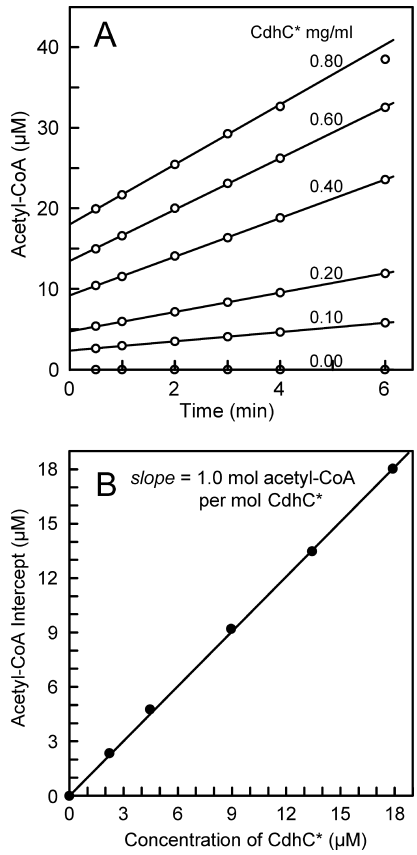

FIGURE 4: Acetyl-CoA synthesis burst. (A) Reactions contained the indicated amounts of β subunit protein (CdhC*) in the presence of 240 μM CO, 50 μM methylcobinamide, 0.1 mM methyl viologen, and 60 μM Ti^{3+} NTA at pH 8.2, and were preincubated for 5 min before the addition of 120 μM CoA at $t = 0$ min. Acetyl-CoA was measured by HPLC analyses of aliquots removed over time, and protein concentration was determined on the basis of one-fourth of the measured iron content. (B) Stoichiometry of enzyme-acetyl formation: a replot of the intercept of acetyl-CoA formed in the burst versus concentration of β subunit protein.

Isolation of an Enzyme-Acetyl Intermediate. In order to obtain direct evidence for the formation of an A cluster-acetyl intermediate, the ACDS β subunit was reacted with methylcobinamide and CO in the absence of CoA and then subjected to gel filtration chromatography. Subsequent addition of CoA to fractions obtained from the column was made in an attempt to capture acetyl groups in the form of acetyl-CoA from any enzyme-acetyl species that may have survived. HPLC analyses were performed to quantify acetyl-CoA and methylcobinamide in the fractions, and spectral analyses allowed for the separate quantification of cob(II)-inamide[3]. As shown in Figure 5, high levels of the enzyme-acetyl intermediate were observed. The total acetyl groups captured, measured by the amounts of acetyl-CoA formed in the fractions, was 109% of the amount of enzyme present, calculated on the basis of absorbance at 400 nm using the value of the absorptivity coefficient of 4466 M^{-1} per Fe atom previously determined from ICP analyses of the recombinant β subunit. A recovery of 90% was estimated assuming that all of the enzyme initially present in the reaction mixture

[3] A separation of the peaks of methylcobinamide and cob(II)inamide on the Superose 12 column is most likely due to adsorptive effects of the matrix because both compounds elute substantially later than the total liquid volume V_t of the column, which is at fractions ~32−34. Residual cob(I)inamide was not detected.

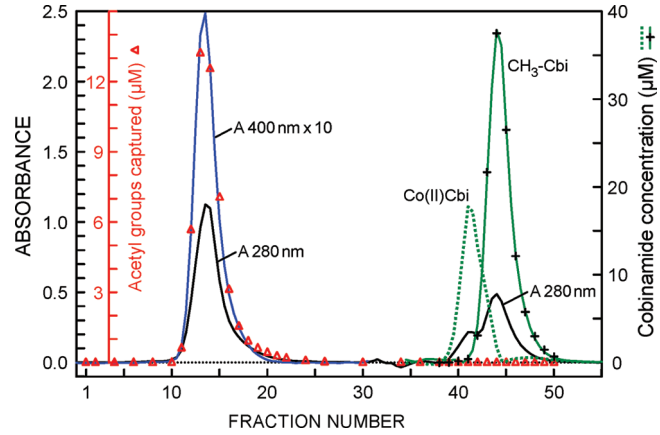

FIGURE 5: Isolation of an A cluster-acetyl intermediate form of the ACDS β subunit. A reaction mixture containing 33 μM ACDS β subunit protein, 100 μM methylcobinamide, and 50 μM $Ti3^+$ NTA was incubated under a 100% CO atmosphere for 5 min and applied to Superose 12 gel filtration column. During fraction collection, CoA was added to each fraction, and subsequent HPLC analysis was used to determine the concentration of acetyl groups captured from the eluted enzyme (Δ, in red). Spectral analyses of methylcobinamide and cob(II)inamide are shown (solid and dashed green lines, respectively), and HPLC results for methylcobinamide are given (+). Absorbance is plotted at 280 nm (black) and 400 nm × 10 (blue), as indicated.

was recovered in the fractions, while a value of 100% was obtained on the basis of the amount of methylcobinamide that was converted to cob(II)cobinamide. Therefore, within the error of analyses, essentially quantitative recovery of the acetyl-enzyme species was obtained. These experiments constitute the first direct isolation of an A cluster enzyme-acetyl intermediate, and the results show that the A cluster-acetyl species is stable under the conditions employed with little or no evidence for hydrolysis.

Uptake of Electrons during Activation of the β Subunit A Cluster and Electron Release upon Reductive Elimination of the Acetyl Group from the A Cluster-Acetyl Intermediate. Under the redox conditions used in the reactions to assess the initial burst formation of acetyl-CoA in Figure 4 (−460 to −470 mV at pH 8.2), only about 5−7% of the enzyme is expected to be present in the reduced active form. However, essentially 100% formation of the A cluster-acetyl species was observed, suggesting that acetyl formation is sufficiently favorable to shift the redox equilibrium and drive the uptake of the required number of electrons (from the partially reduced methyl viologen redox buffer system) needed to activate all of the enzyme molecules for A cluster-acetyl formation. To test this hypothesis, spectrophotometric measurements were made to monitor the changes taking place in the levels of reduced and oxidized methyl viologen in reactions with increasing concentrations of enzyme, performed under conditions identical to those described in Figure 4. During the 5 min preincubation in the presence of all substrates except CoA, the initial absorbance at 600 nm, which was around 0.8 in the absence of enzyme, stabilized at progressively lower values as the amount of β subunit protein was increased, as shown in Figure 6A. Analysis of full UV−visible spectra recorded during this time showed that cob(II)inamide was present in all of the reactions with no evidence for any of the initially produced cob(I)inamide remaining, as expected under the existing redox conditions. Addition of CoA resulted in an immediate large jump in

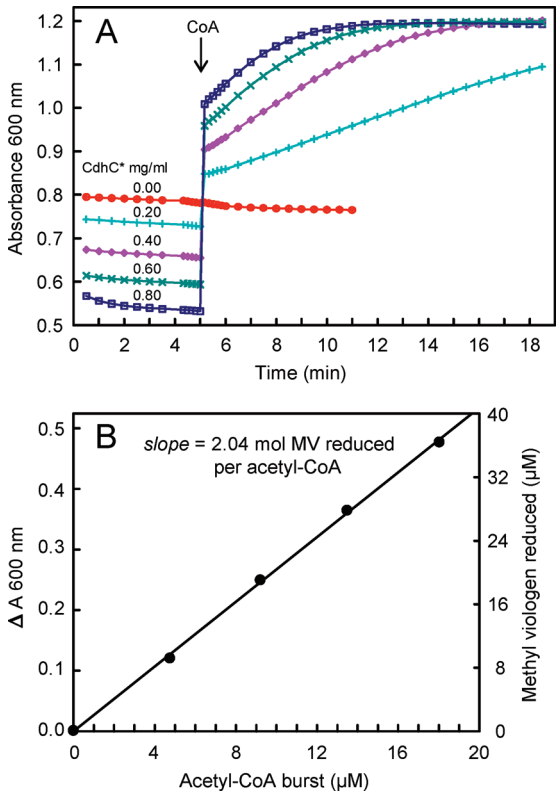

FIGURE 6: Uptake and release of electrons by the ACDS β subunit in the formation of an A cluster-acetyl species and in the reductive elimination of the enzyme-acetyl group. (A) Reactions identical to those in Figure 4 were monitored spectrophotometrically prior to and after the addition of CoA. Data were collected at 30 s intervals except in the region of 4.3 to 6.5 min, where the intervals were set to 10 s. (B) Plot of reduced methyl viologen formed versus the amount of acetyl-CoA produced in the burst.

absorbance, which was followed by a steady increase over time until maximum reduction of the methyl viologen had taken place at an absorbance of around 1.2. Changes in other regions of the spectra during the jump showed evidence for the production of trace amounts of cob(I)inamide (1−2 μM) in the two most highly reduced reactions, but overall the changes observed were almost entirely due to reduction of the methyl viologen (except of course for absorbance due to CoA). The concentration of reduced methyl viologen produced during the jump, calculated from the difference in absorbance at 600 nm immediately before and after addition of CoA, was almost exactly twice the concentration of acetyl-CoA formed in the burst, as shown in the plot in Figure 6B. This result indicated that reductive elimination of the acetyl group from the A cluster-acetyl species was accompanied by the release of two low potential electrons to the viologen buffer system. Since cob(I)inamide is produced during the steady state formation of acetyl-CoA over time, the increase in absorbance that continues after adding CoA, until essentially all of the available methylcobinamide is consumed at the plateau, is interpreted as being due to the reduction of methyl viologen by the product cob(I)inamide as it is formed.

The results also indicated that two electrons are taken up during the activation of the enzyme and formation of the enzyme-acetyl adduct. The extent of decrease in absorbance that occurs as increasing amounts of the enzyme were preincubated corresponded to the net uptake of only one electron from the viologen buffer system, as seen in Figure 6A prior to addition of CoA. However, acetyl group formation on the enzyme is expected to produce an equal amount of cob(I)inamide, which would react to generate a nearly equivalent amount of reduced methyl viologen. Thus, with one equivalent being returned to the redox buffer system under the prevailing redox potentials in the reactions, the results indicate that a total of two electrons were taken up in the activation and formation of the acetyl-enzyme.

DISCUSSION

Requirement for a Base-off Corrinoid as Methyl Donor for Acetyl C−C Bond Formation. The importance of the nature of the methyl group donor for efficient catalysis of acetyl C−C bond formation by the ACDS β subunit protein is evident from a comparison of the high activity of acetyl-CoA synthesis using methylcobinaminde (a base-off methyl corrinoid) versus the low rates detected with a base-on corrinoid such as methylcobalamin. The reaction, eq 6, was approximately 1500 times faster with methylcobinamide (44 min^{-1}) versus methylcobalamin (0.028 min^{-1}), consistent with the substantially higher reactivity for nucleophilic displacement of the methyl group from a base-off corrinoid (*29, 30*).

$$CH_3\text{-Co(III) corrinoid} + CO + CoA \rightleftarrows \text{acetyl-CoA} + \text{Co(I) corrinoid} + H^+ \quad (6)$$

A comparable rate enhancement of ~2000-fold has been observed using the CODH/ACS enzyme (*31*). In that report, methylcobinamide supported acetyl-CoA synthesis at a rate of about 1% of the native corrinoid iron-sulfur protein, which was interpreted as indicating that an additional 100-fold rate enhancement could be due to the interaction of the corrinoid protein with CODH/ACS. In contrast, methylcobinamide afforded maximal turnover rates with the ACDS β subunit, measured here at 25 °C, that were about 10 times higher than those reported for CODH/ACS at 55 °C, and about 30% of the rate observed for acetyl-CoA synthesis by the ACDS complex using its physiological methyl donor substrate CH_3-H_4SPt. These results imply a significantly smaller enhancement due to the protein in the case of the ACDS corrinoid protein subcomponent, on the order of ~3.3-fold. Furthermore, the saturation effects found here suggest that a major role of the corrinoid protein as an integral part of the ACDS complex is to create a high effective concentration of the methyl donor species at the active site of the β subunit. The local concentration achieved could be around 5 mM or higher since this is the level that would give 90% of maximal activity with methylcobinamide. The highly efficient overall synthesis of acetyl-CoA found here, taken together with previous results that show turnover rates of redox dependent acetyl group transfer as high as that of the native ACDS complex (*12*), verify that the recombinant ACDS β subunit protein is a functionally replete A cluster enzyme—a system that reliably represents the core catalytic activity of the ACDS complex acting in isolation from all other protein components.

Redox Requirements for Overall Acetyl-CoA Synthesis and the Quantitative Formation of an A Cluster-Acetyl Species. To date, controlled potential studies on the redox dependence of the catalytic functions of the A cluster have been focused on its activity in catalyzing acetyl group transfer (e.g., CoA exchange activity), which is thought to proceed via the formation of an acetyl-enzyme intermediate (eq 2) (*8, 7*).

Similar experiments on the redox activation of overall acetyl-CoA synthesis have not been attempted, primarily because of the difficulty in maintaining a controlled potential in the presence of CO dehydrogenase in the reactions using CO as a substrate[4]. As shown in Figure 3A, reductive activation of acetyl-CoA synthesis closely conforms to the Nernst equation as an apparent one-electron process. The observed midpoint potential for activation displays a strong pH dependence and becomes more negative by approximately 53 mV/pH unit as the pH is increased (Figure 3B). Earlier studies showed a similar, strong pH dependence for redox activation of acetyl transferase activity of about 40 mV/pH unit (*7*). The midpoint potentials for activation of acetyl-CoA synthesis were slightly less negative than those for the activation of acetyl transferase (by about 20 mV). This could be due to variations in the redox buffer systems employed, the relatively large differences in enzyme concentrations required in the two assays, or other factors such as the presence of additional substrates, and so forth. Nonetheless, the general similarity of the results strongly suggests that reductive activation of the enzyme for acetyl group transfer, as related to C−S bond activation, is in fact the same process that is involved in the overall activation of the enzyme for C−C bond synthesis and cleavage.

Our findings with regard to the short lag phase in reactions that contained no added reducing agent, a lag that can be eliminated entirely by removing traces of an oxidant present in the CoA solution, are readily interpreted as being due to rapid autoactivation of the system by the product cob(I)inamide. Thus, only a small fraction of active enzyme molecules would be needed in order to catalyze sufficient Co(I) production to quickly reduce the entire population. This could also explain the significant, although somewhat meager, degree of turnover observed with the recombinant bacterial ACS protein in samples made "reductant free" in the presence of the methylated corrinoid protein (*32*).

Although previous kinetic experiments on acetyl transfer implicate an enzyme-acetyl intermediate, presumably formed by the reaction of acetyl-CoA with a reduced nucleophilic form of the A cluster, there have been no other direct measurements made to permit the characterization of the A cluster-acetyl species. The burst formation of acetyl-CoA, shown in Figure 4, strongly indicates that stoichiometric levels of the enzyme-acetyl intermediate are formed by the reaction of the β subunit with substrates CO and methylcobinamide in the absence of CoA. Indeed, essentially complete conversion of the enzyme to an acetylated form was demonstrated directly by the chromatographic isolation shown in Figure 5, with the generation of an enzyme-acetyl species sufficiently stable to be isolated and still capable of rapidly reacting with CoA to produce acetyl-CoA. Thus, the results presented here provide the most compelling evidence to date for the quantitative formation of a stable A cluster-acetyl derivative.

Two Low Potential Electrons in the Activation of the β Subunit A Cluster. The A cluster-acetyl adduct can be viewed as both the proximate species to undergo C−C bond cleavage as well as the immediate product to arise from C−C bond formation. Hence, a detailed knowledge of the properties of this species is highly relevant to the understanding of the process of acetyl C−C bond activation. Direct spectrophotometric analysis of the uptake and release of electrons by the β subunit protein in reactions involving stoichiometric formation of the A cluster-acetyl derivative and its subsequent reaction with CoA, shown in Figure 6, establish that two low potential electrons are involved. Therefore, in the reductive activation of the A cluster, the one-electron Nernst behavior can be interpreted as the result of two separate one-electron processes, both taking place at a very low redox potential. However, even under relatively mild reducing potentials, the reaction of the enzyme with CO and methylcobinamide goes to completion, quantitatively converting the enzyme into the A cluster-acetyl form. As described by eq 7, the sequence of events taking place under weakly reducing potentials above the $Co^{2+/1+}$ cobinamide midpoint would involve the reduction of the enzyme by two one-electron steps followed by reaction with substrates to form the enzyme-acetyl intermediate. Although reduction of the

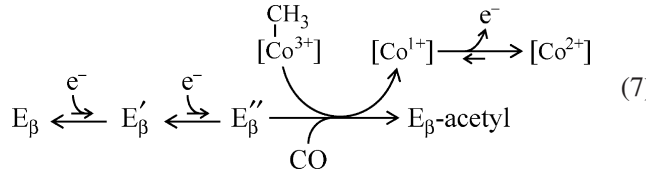

(7)

enzyme is unfavorable, and only a small fraction of the enzyme is expected to be in the fully active E_β'' form, it is evident that the formation of the acetyl species is a highly favorable process. The results indicate that spontaneous formation of the enzyme-acetyl, along with the oxidation of the Co^{1+} cobinamide product under mild reducing conditions, shifts the equilibrium to convert essentially all of the enzyme into the enzyme-acetyl form. With a $Co^{2+/1+}$ cobinamide midpoint potential significantly more negative than that of the methyl viologen $MV_{ox}/MV^{\bullet+}$ couple, one of the two electrons originally taken up to activate the enzyme is subsequently returned to the redox buffer system by oxidation of the cob(I)inamide product released in the formation of the E_β-acetyl species. Thus, two low potential electrons are "trapped" in the process of the formation of the enzyme-acetyl intermediate. Under physiological redox potentials in vivo, this mechanism may allow for extensive activation of the enzyme at potentials much less negative than otherwise required to fully reduce the enzyme.

Equation 8 describes the reaction sequence taking place upon addition of CoA to the enzyme-acetyl species. The burst

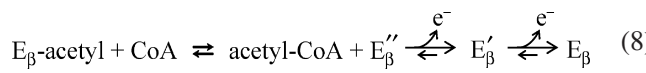

(8)

of acetyl-CoA is stoichiometric with the enzyme, and two low potential electrons are rapidly released from the reduced enzyme to the relatively oxidizing environment. The data from Figure 6 indicate that the rate of reoxidation of the enzyme under conditions of ca. −460 to −470 mV is at least 50 times greater (lower limit) than the steady state rate of acetyl-CoA synthesis and that a constant rate of turnover is quickly established upon release of the fully reduced enzyme

[4] The CODH activities in CODH/ACS and in ACDS preparations are overwhelming; however, even traces of CODH, if present in purified dissociated fractions, can result in strong, uncontrolled reduction of reaction mixtures because of the very high specific activity of the CODH enzymes. The purified recombinant β subunit has no detectable CODH activity, and there is no evidence that *E. coli* contains CO dehydrogenase.

E_β'' by reaction of the E_β-acetyl species with CoA. Overall, the results are consistent with rapid redox equilibration of the isolated β subunit protein, both during the initial reduction of the enzyme by the viologen buffer system, and in the process of reoxidation.

Reaction Mechanism. A knowledge of the redox states of nickel and iron in the reduced nucleophilic form of the A cluster is valuable in efforts to elucidate the mechanism of acetyl C−C bond synthesis and cleavage. The results presented here argue against one-electron reduced forms such as $[Fe_4S_4]^{2+}$-Ni_p^{1+} or $[Fe_4S_4]^{1+}$-Ni_p^{2+} as species representing the active fully reduced form of the A cluster. Two-electron reduction of Ni_p^{2+} to the Ni_p^{0} state has been considered (*10, 18, 32*); however, density functional theory calculations point out that Ni_p^{0} is not stable next to an oxidized Fe/S cluster in a form such as $[Fe_4S_4]^{2+}$-Ni_p^{0} (*24, 20*). The theoretically more stable three-electron reduced form $[Fe_4S_4]^{1+}$-Ni_p^{0} is, nevertheless, also inconsistent with the present finding that reduction proceeds by two electrons. Species such as Ni_p^{3+}-methyl or Ni_p^{3+}-acetyl, potentially formed by nucleophilic attack of Ni_p^{1+}, would require only a relatively weak one-electron reductant to be converted to the corresponding Ni_p^{2+} adducts (*12*). But this mechanism, or others in which one weakly reducing equivalent would remain associated with the enzyme, is at odds with a situation in which both electrons exhibit low potential characteristics.

Formally, a one-electron reduction to the Ni_p^{1+} state might be all that is required for acetyl transfer/CoA exchange via a transiently formed Ni_p^{3+}-acetyl species without the involvement of a second electron. However, this is difficult to rationalize if it is considered that the activation of overall acetyl-CoA synthesis activity (involving two electrons) in all likelihood is exactly the same process that is used in the activation of acetyl transfer activity. A mechanism involving the shuttling of one electron back and forth during the reaction cycle from a source outside of the A cluster has been proposed (*33, 22*). If this is correct, then the two-electron reduced form of the A cluster would have to be generated precisely at the instant that an acetyl-Ni or a methyl-Ni bond is established. Such a requirement seems less probable on kinetic grounds than one in which both electrons would be already associated with the active center.

Data from Fe K-edge X-ray absorption spectroscopic studies (*13*) and Mössbauer analyses (*32*) on A cluster enzymes reduced with Ti^{3+} citrate indicate that a significant population of the Fe/S clusters is able to achieve the $[Fe_4S_4]^{1+}$ state. In addition, Ni XANES and Ni L-edge spectroscopy (*13, 14*) indicate that a substantial amount of a species ascribed to Ni^{1+} is formed as well. Thus, we consider $[Fe_4S_4]^{1+}$-Ni_p^{1+} as a reasonable designation for the Fe/S cluster and Ni_p valence states in the two-electron reduced form of the A cluster, and such an arrangement could provide an effective means to accommodate two low potential electrons in a delocalized system. As depicted in Scheme 2A, the nucleophilic attack of a $[Fe_4S_4]^{1+}$-Ni_p^{1+} species on the methyl group of methylcobinamide would generate directly a methyl-Ni_p^{2+} enzyme intermediate. In the next step, reaction of the methyl-Ni_p^{2+} species with carbon monoxide (carbonylation) would form an acetyl-Ni_p^{2+} species, the enzyme-acetyl intermediate. Reaction of the acetyl-Ni_p^{2+} species with CoA, in the third step, would produce acetyl-CoA and regenerate the fully reduced enzyme. A mechanism in which CO adds before

Scheme 2: Reaction Mechanism Involving the Two-Electron Reduced A Cluster as Either (A) a $[Fe_4S_4]^{1+}$-Ni_p^{1+} Species or (B) a $[Fe_4S_4]^{2+}$-Ni_p^{2+}-Hydride

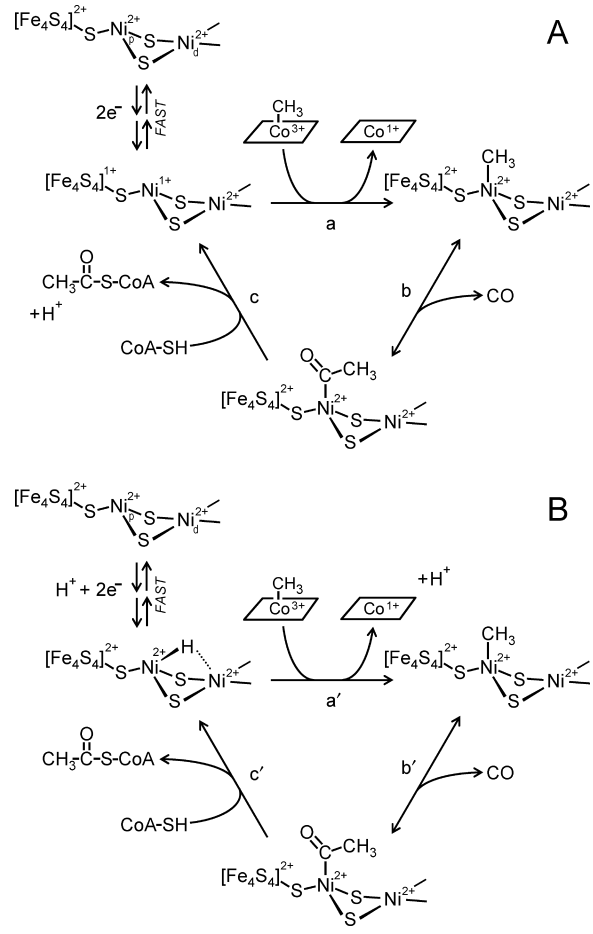

methyl, in the order proposed by Ragsdale and co-workers (*34*), cannot be excluded by the results presented here. Although carbonylation of biologically relevant methyl-Ni^{2+} complexes is well established (*35, 36*) and methylation of a zero-valent Ni-carbonyl adduct by methyl-Co^{3+} is unlikely (*37*), new findings from pulse−chase experiments on CODH/ACS indicate that both CO and methyl groups bound to the enzyme exhibit a high commitment to catalysis, with the surprising implication of a random mechanism (*38*). Here, we have chosen to write only the sequence in which addition of a methyl group precedes the reaction with CO.

In Scheme 2A, both electrons in the $[Fe_4S_4]^{1+}$-Ni_p^{1+} configuration are implied to react in concert in the process of nucleophilic attack on methyl and acetyl donor substrates. This would require a shift of electron density from the Fe/S center toward Ni_p concomitant with methyl−Ni bond formation, and such attendant electron transfer is expected to be rapid due to the short distance involved. In a delocalized $[Fe_4S_4]^{1+}$-Ni_p^{1+} arrangement, it seems likely that some degree of nucleophilic reactivity is traded for stability, as needed to achieve a two-electron reduced form. This view is supported by the marginal base-on methyl corrinoid reactivity and a midpoint potential for A cluster reduction that falls within a region generally matching that of the base-off corrinoid $Co^{2+/1+}$ couple.

There are substantial differences between the archaeal ACDS β subunit system and the bacterial ACS α protein that may prevent direct comparison of some results. Along

with major variations in molecular masses and amino acid sequences of the two proteins, such differences include the apparent lack of detectable high-spin Ni^{2+} in the bacterial enzyme by Mössbauer analysis, as compared with the as-isolated ACDS β subunit in which roughly 50% of the enzyme Ni^{2+} is observed in the high-spin state by Ni L-edge experiments (*32, 14*). In addition, the high levels of activity, and the quantitative stoichiometric formation of an A cluster-acetyl intermediate found here with the recombinant ACDS β subunit stand in contrast with the marked structural and functional heterogeneity that has been characterized in the bacterial ACS α protein (*32, 39* and references therein). Interestingly, no evidence for a $[Fe_4S_4]^{1+}$-Ni_p^{1+} configuration was found in Mössbauer studies on the bacterial α subunit (*32*). However, as pointed out in that paper, the reduction potentials of the Fe/S and Ni_p subcomponents may be strongly influenced by different protein conformational states that are hard to assess. If so, this could have major effects on how the two electrons are distributed between the Fe/S and Ni_p subcenters, either allowing or disallowing access to the $[Fe_4S_4]^{1+}$-Ni_p^{1+} state.

On the basis of previous acetyl transferase data (*7, 12*) and from the maximum turnover found here with saturating methylcobinamide under fully reducing conditions, the rate of acetyl transfer from the enzyme to CoA (Scheme 2, reaction c) can be estimated to be at least 100 times greater than the steady state rate of acetyl-CoA synthesis under comparable reaction conditions. Since transfer of the acetyl group to CoA is fast, either methyl group transfer to the enzyme or the insertion of CO to generate the acetyl intermediate (Scheme 2, reactions a or b) would be rate limiting overall. Although direct kinetic measurements on the CO insertion reaction have not been described, it is suggested to be the slow step by presteady state experiments with bacterial ACS in which the reaction was monitored indirectly using methyl group transfer to the corrinoid iron-sulfur protein as a reporter (*40*). Because redox equilibration of the ACDS β subunit enzyme is rapid, the rate of acetyl-CoA synthesis under weakly reducing conditions in which most of the enzyme remains in the oxidized form would be limited either by the concentration of the fully reduced enzyme or by the amount of enzyme present in the methylated form. In the latter case, a low level of the methylated enzyme would result from equilibrium methylation of a low concentration of the fully reduced form.

Role of Protonation. At present, little is known about the factors involved in stabilizing the enzyme in its activated reduced form. As mentioned above, it is unclear how a $[Fe_4S_4]^{2+}$-Ni_p^{0} species could be a major contributor to the stability of the two-electron reduced A cluster. The evidence presented here and in ref *7* strongly points to a step involving the uptake of a proton as being required to generate the reduced nucleophilic species. Exactly how protonation helps to stabilize the reduced A cluster is currently unknown. One simple interpretation is that protonation of a ligand assists in the formation of a lower Ni_p valence state. Protonation of one of the bridging cysteine thiolates might be used as a means to further deactivate thiolate coordination to Ni_p. The interruption of S coordination to Ni_p rather than to Ni_d would be invoked because a protonated thiolate (thiol) also coordinated by Ni_d should be maximally deactivated with respect to Ni_p. In general, however, competition of a proton with two Ni ions is unfavorable, especially at neutral pH and with both metals in the oxidized state. A second option would be the protonation of a ligand involved in Fe/S coordination to alter the redox potential of the Fe/S cluster. This could be particularly important in a mechanism requiring $[Fe_4S_4]^{1+}$-Ni_p^{1+} as the active nucleophile.

A third alternative would involve the stabilization of Ni_p^0 by direct conversion into a Ni^{2+}-hydride, as indicated in eq 9.

$$[Fe_4S_4]^{1+}\text{-}Ni_p^{1+} \rightleftarrows [Fe_4S_4]^{2+}\text{-}Ni_p^{0} \overset{H^+}{\rightleftharpoons} [Fe_4S_4]^{2+}\text{-}Ni_p^{2+}\text{-}H \quad (9)$$

In this case, participation of the Fe/S cluster would differ markedly from the situation depicted in Scheme 2A, and the role of the distal Ni could take on additional significance. The difficulty in forming a stable Ni_p^0 state in the absence of a strong π acceptor ligand (e.g., CO or phosphine), and the problem of maintaining coordination of Ni_p^0 by ligands such as thioether or metal-deactivated thiolates would be mitigated in the case of a Ni^{2+}-hydride. Precedent for a greater stability of the hydride exists from studies on a mononuclear Ni complex model of the A cluster involving thioether ligation, which was significantly more stable in the form of a Ni^{2+}-hydride than as a complex containing Ni^0 (*35, 36*). In that work, it was also established that such hydrides are reactive toward electron-deficient carbon and are capable of yielding Ni^{2+}-alkyl species. In a recent report on a Ru−Ni complex with catalytic activity mimicking hydrogenase, a Ni^{2+}-hydride species was identified in which H^- is located in a position bridging between Ni and Ru (*41*). The structure of that complex is relevant to the A cluster, since it also contains a "distal" Ni^{2+} site in square-planar N_2S_2 coordination and a "proximal" metal in a distorted or nonclassical geometry sharing both of the square-planar Ni-thiolate ligands. The Ni−Ni distance in the A cluster, which appears to shorten upon reduction (*13*), is such that it too might reasonably accommodate a bridging hydride, thus a more dynamic role of Ni_d other than simply to deactivate the thiolate ligands to Ni_p is conceivable.

A mechanism for acetyl-CoA synthesis involving the participation of a Ni^{2+}-hydride species is depicted in Scheme 2B. In contrast to other schemes in which little or no direct attention has been paid to proton transfer steps, a role for protonation in stabilization of the reduced form of the A cluster is shown here explicitly, along with consequences for subsequent proton release in the catalytic cycle. In the mechanism involving a hydride, liberation of a proton would take place at a different step than in a nonhydride scheme, specifically in the process of attack of the Ni_p^{2+}-hydride on the corrinoid methyl group in reaction a′. The hydride attack on the thioester group of acetyl-CoA, in the reverse of reaction c′, would liberate CoA as a thiol, rather than a thiolate. This might be reflected in the pH optimum, which is below pH 7 for the CoA exchange reaction, where CoA exists mainly as the thiol. A better knowledge of the step at which protons are released will help distinguish whether or not a Ni^{2+}-hydride species takes part in catalysis. Experiments are underway to test for hydride formation and to characterize differences in the pH requirements of individual steps in the catalytic cycle.

SUPPORTING INFORMATION AVAILABLE

A description of the experimental methods and the redox potentials obtained by addition of aliquots of Ti^{3+} NTA to mixtures containing methyl viologen and benzyl viologen is provided, with Figure S1 showing the observed potentials fit to the Nernst equation. Primary plots of acetyl-CoA formation versus reaction time at different pH and redox potentials are shown in Figure S2, with an initial burst of acetyl-CoA noticeable under all conditions examined. This material is available free of charge via the Internet at http://pubs.acs.org.

REFERENCES

1. Ferry, J. G. (1999) Enzymology of one-carbon metabolism in methanogenic pathways. *FEMS Microbiol. Rev. 23*, 13–38.
2. Grahame, D. A. (2003) Acetate C-C bond formation and decomposition in the anaerobic world: The structure of a central enzyme and its key active site metal cluster. *Trends Biochem. Sci. 28*, 221–224.
3. Dai, Y.-R., Reed, D. W., Millstein, J. H., Hartzell, P. L., Grahame, D. A., and DeMoll, E. (1998) The acetyl-CoA decarbonylase/synthase complex from *Archaeoglobus fulgidus*: purification, characterization, and properties. *Arch. Microbiol. 169*, 525–529.
4. Grahame, D. A. (1991) Catalysis of acetyl-CoA cleavage and tetrahydrosarcinapterin methylation by a carbon monoxide dehydrogenase-corrinoid enzyme complex. *J. Biol. Chem. 266*, 22227–22233.
5. Grahame, D. A., and DeMoll, E. (1995) Substrate and accessory protein requirements and thermodynamics of acetyl-CoA synthesis and cleavage in *Methanosarcina barkeri*. *Biochemistry 34*, 4617–4624.
6. Grahame, D. A., and DeMoll, E. (1996) Partial reactions catalyzed by protein components of the acetyl-CoA decarbonylase/synthase enzyme complex from *Methanosarcina barkeri*. *J. Biol. Chem. 271*, 8352–8358.
7. Bhaskar, B., DeMoll, E., and Grahame, D. A. (1998) Redox dependent acetyl transfer partial reaction of the acetyl-CoA decarbonylase/synthase complex: Kinetics and mechanism. *Biochemistry 37*, 14491–14499.
8. Lu, W. P., and Ragsdale, S. W. (1991) Reductive activation of the coenzyme A/acetyl-CoA isotopic exchange reaction catalyzed by carbon monoxide dehydrogenase from *Clostridium thermoaceticum* and its inhibition by nitrous oxide and carbon monoxide. *J. Biol. Chem. 266*, 3554–3564.
9. Doukov, T. I., Iverson, T. M., Seravalli, J., Ragsdale, S. W., and Drennan, C. L. (2002) A Ni-Fe-Cu center in a bifunctional carbon monoxide dehydrogenase/acetyl-CoA synthase. *Science 298*, 567–572.
10. Darnault, C., Volbeda, A., Kim, E. J., Legrand, P., Vernède, X., Lindahl, P. A., and Fontecilla-Camps, J. C. (2003) Ni-Zn-[Fe_4S_4] and Ni-Ni-[Fe_4S_4] clusters in closed and open α subunits of acetyl-CoA synthase/carbon monoxide dehydrogenase. *Nat. Struct. Biol. 4*, 271–279.
11. Svetlitchnyi, V., Dobbek, H., Meyer-Klaucke, W., Meins, T., Thiele, B., Romer, P., Huber, R., and Meyer, O. (2004) A functional Ni-Ni-[4Fe-4S] cluster in the monomeric acetyl-CoA synthase from *Carboxydothermus hydrogenoformans*. *Proc. Natl. Acad. Sci. U.S.A. 101*, 446–451.
12. Gencic, S., and Grahame, D. A. (2003) Nickel in subunit β of the acetyl-CoA decarbonylase/synthase multienzyme complex in methanogens: Catalytic properties and evidence for a binuclear Ni-Ni site. *J. Biol. Chem. 278*, 6101–6110.
13. Gu, W., Gencic, S., Cramer, S. P., and Grahame, D. A. (2003) The A-cluster in subunit β of the acetyl-CoA decarbonylase/synthase complex from *Methanosarcina thermophila*: Ni and Fe K-edge XANES and EXAFS analyses. *J. Am. Chem. Soc. 125*, 15343–15351.
14. Funk, T., Gu, W., Friedrich, S., Wang, H., Gencic, S., Grahame, D. A., and Cramer, S. P. (2004) Chemically distinct Ni sites in the A cluster in subunit β of the acetyl-CoA decarbonylase/synthase complex from *Methanosarcina thermophila*: Ni L-edge and X-ray magnetic circular dichroism analyses. *J. Am. Chem. Soc. 126*, 88–95.
15. Raybuck, S. A., Bastian, N. R., Orme-Johnson, W. H., and Walsh, C. T. (1988) Kinetic characterization of the carbon monoxide-acetyl-CoA (carbonyl group) exchange activity of the acetyl-CoA synthesizing CO dehydrogenase from *Clostridium thermoaceticum*. *Biochemistry 27*, 7698–7702.
16. Tucci, G. C., and Holm, R. H. (1995) Nickel-mediated formation of thioesters from bound methyl, thiols, and carbon monoxide: A possible reaction pathway of acetyl-coenzyme A synthase activity in nickel-containing carbon monoxide dehydrogenases. *J. Am. Chem. Soc. 117*, 6489–6496.
17. Hegg, E. L. (2004) Unraveling the structure and mechanism of acetyl-coenzyme A synthase. *Acc. Chem. Res. 37*, 775–783.
18. Lindahl, P. A. (2004) Acetyl-coenzyme A synthase: the case for a Ni_p^0-based mechanism of catalysis. *J. Biol. Inorg. Chem. 9*, 516–524.
19. Webster, C. E., Darensbourg, M. Y., Lindahl, P. A., and Hall, M. B. (2004) Structures and energetics of models for the active site of acetyl-coenzyme A synthase: Role of distal and proximal metals in catalysis. *J. Am. Chem. Soc. 126*, 3410–3411.
20. Amara, P., Volbeda, A., Fontecilla-Camps, J. C., and Field, M. J. (2005) A quantum chemical study of the reaction mechanism of acetyl-coenzyme A synthase. *J. Am. Chem. Soc. 127*, 2776–2784.
21. Riordan, C. G. (2004) Synthetic chemistry and chemical precedents for understanding the structure and function of acetyl-coenzyme A synthase. *J. Biol. Inorg. Chem. 9*, 542–549.
22. Ragsdale, S. W. (2007) Nickel and the carbon cycle. *J. Inorg. Biochem. 101*, 1657–1666.
23. George, S. J., Seravalli, J., and Ragsdale, S. W. (2005) EPR and infrared spectroscopic evidence that a kinetically competent paramagnetic intermediate is formed when acetyl-coenzyme A synthase reacts with CO. *J. Am. Chem. Soc. 127*, 13500–13501.
24. Schenker, R. P., and Brunold, T. C. (2003) Computational studies on the A cluster of acetyl-coenzyme A synthase: Geometric and electronic properties of the NiFeC species and mechanistic implications. *J. Am. Chem. Soc. 125*, 13962–13963.
25. Graentzdoerffer, A., Rauh, D., Pich, A., and Andreesen, J. R. (2003) Molecular and biochemical characterization of two tungsten- and selenium-containing formate dehydrogenases from *Eubacterium acidaminophilum* that are associated with components of an iron-only hydrogenase. *Arch. Microbiol. 179*, 116–130.
26. Zou, X., Evans, D. R., and Brown, K. L. (1995) Efficient and convenient method for axial nucleotide removal from vitamin B_{12} and its derivatives. *Inorg. Chem. 34*, 1634–1635.
27. Jacobsen, D. W., Green, R., and Brown, K. L. (1986) Analysis of cobalamin coenzymes and other corrinoids by high-performance liquid chromatography. *Methods Enzymol. 123*, 14–22.
28. Hogenkamp, H. P. C., and Holmes, S. (1970) Polarography of cobalamins and cobinamides. *Biochemistry 9*, 1886–1892.
29. Norris, P. R., and Pratt, J. M. (1996) Methyl transfer reactions of protein-free Co corrinoids. *BioFactors 5*, 240.
30. Pratt, J. M. (1999) The Roles of Co, Corrin, and Protein. I. Co-Ligand Bonding and the Trans Effect, in *Chemistry and Biochemistry of B_{12}* (Banerjee, R., Ed.) Vol. 1, pp 73−112, John Wiley and Sons, Inc., New York.
31. Seravalli, J., Brown, K. L., and Ragsdale, S. W. (2001) Acetyl coenzyme A synthesis from unnatural methylated corrinoids: requirement for "base-off" coordination at cobalt. *J. Am. Chem. Soc. 123*, 1786–1787.
32. Bramlett, M. R., Stubna, A., Tan, X., Surovtsev, I. V., Münck, E., and Lindahl, P. A. (2006) Mössbauer and EPR study of recombinant acetyl-CoA synthase from *Moorella thermoacetica*. *Biochemistry 45*, 8674–8685.
33. Ragsdale, S. W. (2004) Life with carbon monoxide. *Crit. Rev. Biochem. Mol. Biol. 39*, 165–195.
34. George, S. J., Seravalli, J., and Ragsdale, S. W. (2005) EPR and infrared spectroscopic evidence that a kinetically competent paramagnetic intermediate is formed when acetyl-coenzyme A synthase reacts with CO. *J. Am. Chem. Soc. 127*, 13500–13501.
35. Stavropoulos, P., Carrie, M., Muetterties, M. C., and Holm, R. H. (1990) Reaction sequence related to that of carbon monoxide dehydrogenase (acetyl coenzyme A synthase): Thioester formation mediated at structurally defined nickel centers. *J. Am. Chem. Soc. 112*, 5385–5387.
36. Stavropoulos, P., Muetterties, M. C., Carrie, M., and Holm, R. H. (1991) Structural and reaction chemistry of nickel complexes in relation to carbon monoxide dehydrogenase: A reaction system simulating acetyl-coenzyme A synthase activity. *J. Am. Chem. Soc. 113*, 8485–8492.

37. Eckert, N. A., Dougherty, W. G., Yap, G. P., and Riordan, C. G. (2007) Methyl transfer from methylcobaloxime to (triphos)Ni(P-Ph_3): Relevance to the mechanism of acetyl coenzyme A synthase. *J. Am. Chem. Soc. 129*, 9286–9287.
38. Seravalli, J., and Ragsdale, S. W. (2008) Pulse chase studies of the synthesis of acetyl-coenzyme A by carbon monoxide dehydrogenase/acetyl-coenzyme A synthase: Evidence for a random mechanism of methyl and carbonyl addition. *J. Biol. Chem. 283*, 8384–8394.
39. Tan, X., Kagiampakis, I., Surovtsev, I. V., Demeler, B., and Lindahl, P. A. (2007) Nickel-dependent oligomerization of the alpha subunit of acetyl-coenzyme A synthase/carbon monoxide dehydrogenase. *Biochemistry 46*, 11606–11613.
40. Tan, X., Surovtsev, I. V., and Lindahl, P. A. (2006) Kinetics of CO insertion and acetyl group transfer steps, and a model of the acetyl-CoA synthase catalytic mechanism. *J. Am. Chem. Soc. 128*, 12331–12338.
41. Ogo, S., Kabe, R., Uehara, K., Kure, B., Nishimura, T., Menon, S. C., Harada, R., Fukuzumi, S., Higuchi, Y., Ohhara, T., Tamada, T., and Kuroki, R. (2007) A dinuclear Ni(μ-H)Ru complex derived from H_2. *Science 316*, 585–587.

BI7024035